Sintering characteristics of nanocrystalline ZnO

X. J. QIN
Key Laboratory of Metastable Materials Science and Technology, Yanshan University, Qinhuangdao, 066004, People's Republic of China; College of Environmental and Chemical Engineering, Yanshan University, Qinhuangdao, 066004, People's Republic of China

G. J. SHAO
College of Environmental and Chemical Engineering, Yanshan University, Qinhuangdao, 066004, People's Republic of China

R. P. LIU*
Key Laboratory of Metastable Materials Science and Technology, Yanshan University, Qinhuangdao, 066004, People's Republic of China
E-mail: riping@ysu.edu.cn

W. K. WANG
Key Laboratory of Metastable Materials Science and Technology, Yanshan University, Qinhuangdao, 066004, People's Republic of China; Institute of Physics, Chinese Academy of Sciences, Beijing, 100080, People's Republic of China

Zinc oxide ceramics have been widely utilized for electrical and electronic devices because of their non-linear current-voltage properties. The non-linear coefficient of zinc oxide ceramics has been found to be the biggest in all semiconductor materials. In the past years, there were a number of studies addressing the sintering and grain growth of coarse crystalline ZnO [1–5]. It was found that the physical properties are directly related to grain size as well as the quantity of grain boundaries. For instance, ZnO ceramics with smaller grain sizes exhibit the larger breakdown voltages. It was reported that nanocrystalline ZnO was characterized by better nonlinear current-voltage properties and can be sintered at much lower temperatures [6, 7]. Unfortunately, less effort has been paid to the growth behavior of nanocrystals during sintering. In this work, control of the grain size of sintered ZnO samples and the growth kinetics during the sintering process of nanocrystalline ZnO are reported.

The nanocrystalline ZnO powders used in the present experiments were produced by the homogeneous precipitation method described elsewhere [8]. The powders, ranging in size from 10 to 30 nm, were ground for 0.5 h in an agate mortar and compacted into disks, 8 mm in diameter and 2 mm in thickness, at a pressure of 750 MPa. The green disks were 0.3 g in weight and had a density of about 48% of the theoretical value. In all experiments, a furnace was raised to the predetermined temperature. The specimen was preheated in the cooler part of the furnace for about 5 min and was then gradually inserted until it was directly below a thermocouple. The specimen was equilibrated with the furnace temperature in 1.5 to 2 min after insertion. The compacted disks were then isothermally sintered at different temperatures 973, 1073 and 1173 K and for various times, from 0.5 to 5 h. Then, the samples was quenched in air.

X-ray diffraction measurements of the samples before and after sintering were conducted with a MDI/JADE5 diffractometer with a Cu Kα radiation source. The grain sizes were calculated according to the width at half height of the diffraction peaks using the Scherrer formula. Microstructures of the samples were examined using a XL30S-FEG field emission gon scanning electron microscope. The density of the samples was obtained using Archimedes principle and ethanol as the immersion fluid.

Relative densities of the samples are shown in Fig. 1. The initial relative density of the compacted sample before sintering is 48% of the theoretical density, which is 5.67 g/cm^3. The effect of sintering time on the densities at different temperatures shows essentially the same tendency. Within 0.5 h, the relative densities of the samples increased rapidly to around 90% for the three sintering temperatures, which is different from the sintering of coarse crystalline ZnO. This is named as the first stage in the present article. In the first stage, densification was fast and the temperature influence was not evident in the present case. The reasons that caused the rapid increasing of the densities are probably shrinkage because of the large porosity of the green bodies, pore collapse, boundary or surface diffusion, etc. [9]. It is in fact not clear which is the most important one. But one thing is clear that it was not caused by grain growth, because the grain size is around 28 nm, which is slightly larger than that of the original grain size, 20 nm. Following the first stage comes the second stage, from 0.5 to 1 h, with the relative densities decreased apparently. The reason was probably that the surfactants adsorbed on the surfaces of the
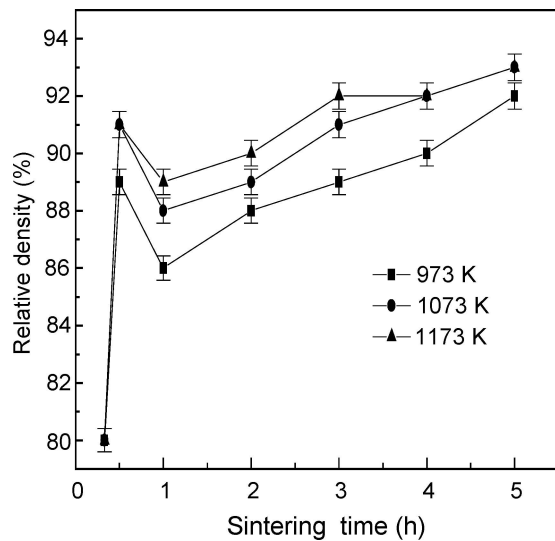
Figure 1 Effect of sintering time on relative density of samples sintered at 973, 1073 and 1173 K respectively.

nano-particles vaporized and led to increase of the porosity. Relative densities of the samples after sintering for 1 h, which is the third stage, show continuous increase with increasing the sintering temperature and time, but the increase rate is much smaller than that in the first stage. The gradual increase of density in the third stage is, not like in the first stage, clearly related to crystal growth. Sintering after 5 h did not cause evident increase in density.

Fig. 2 shows the microstructures of the samples sintered at 973 K for different times. Even from the first glance at the microstructures, it can be seen that the average grain size does not change apparently. Considering the slightly increase of the den-

sity, appropriately extending the sintering time is helpful for improving the quality of the sintered samples. And the morphologies of the particles tend to be rounded.

Fig. 3 shows the microstructures of the samples sintered for 3 h at different temperatures. It can be seen that the average grain size increases rapidly with increasing the sintering temperature, implying the grain growth is more sensitive to temperature than time. At 1173 K, large and faceted crystals with an evident size scattering are formed. Faceted morphologies are typical for growth of germanium, silicon, oxides, compounds, etc. [10–13]. In order to give a better understanding of the grain growth behavior during the sintering, analyses of the growth kinetics are necessary.

Based on the phenomenological kinetic grain growth equation [14]:

$$G^n = Dt \exp\left(-\frac{E}{RT}\right) \qquad (1)$$

Where G is the average grain size at time t, n is the grain growth kinetic exponent, D is the pre-exponential constant for the material, E is the apparent activation energy, R is the gas constant, and T is the absolute temperature.

Equation 1 can be changed into the following form:

$$\log G = \frac{1}{n}\log t + \frac{1}{n}\left[\log D - 0.434\frac{E}{RT}\right] \qquad (2)$$

From the slope of the line of log G versus logt, which is $1/n$, the grain growth kinetic exponent is readily determined. Fig. 4 illustrates the results for the samples
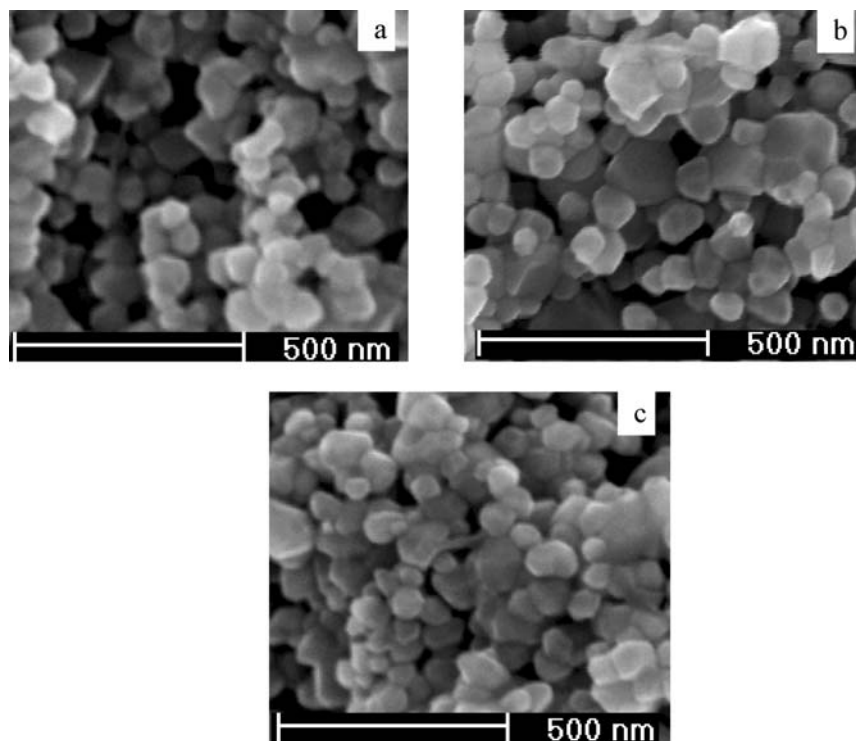

Figure 2 Field emission scanning electron microscope observation of the fractured sections of ZnO nanocrystalline samples sintered at 973 K (a) for 2 h with a mean grain size of 60 nm and relative density of 88%, (b) for 3 h with a mean grain size of 65 nm and relative density of 89%, and (c) for 5 h with a mean grain size of 70 nm and relative density of 92%.
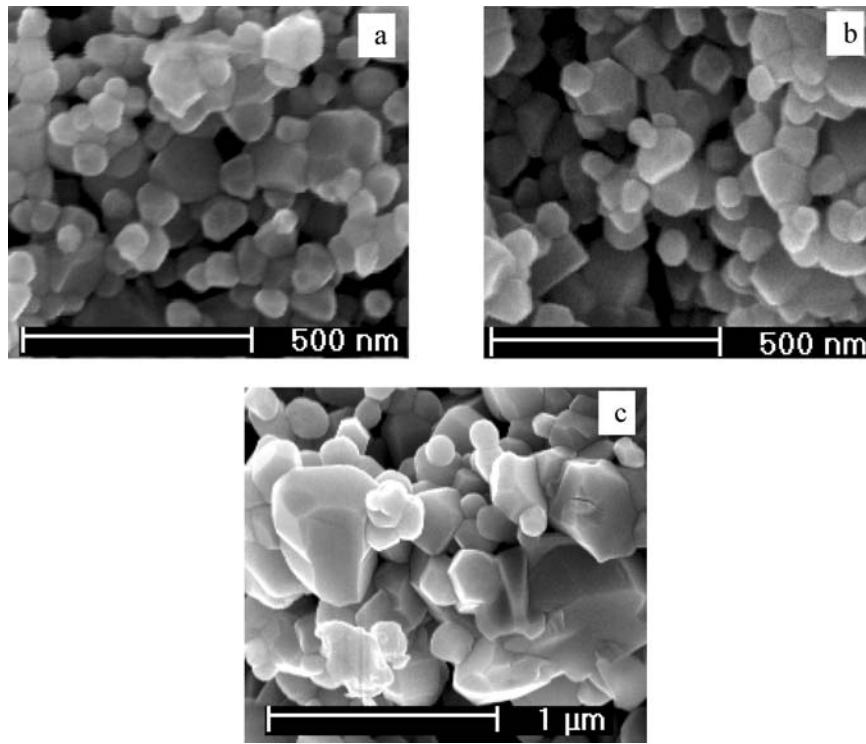
Figure 3 Field emission scanning electron microscope observation of the fractured sections of ZnO nanocrystalline samples sintered for 3 h at (a) 973 K with a mean grain size of 70 nm and relative density of 89%, (b) 1073 K with a mean grain size of 75 nm and relative density of 91%, and (c) 1173 K with a mean grain size of 130 nm and relative density of 93%.
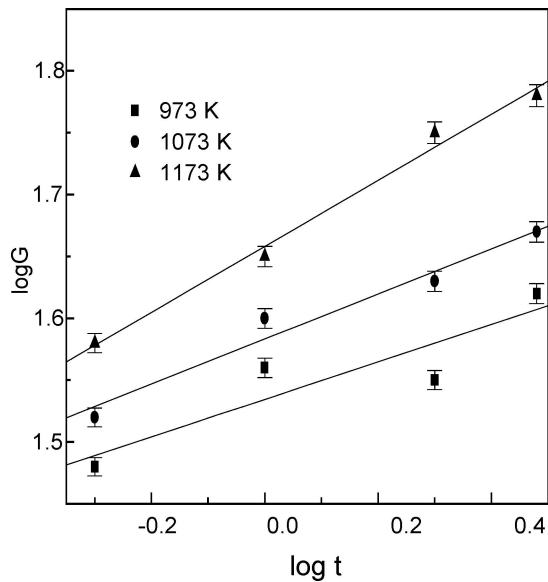

Figure 4 Grain size G versus time t for growth of nanocrystalline ZnO sintered at three different temperatures.

Figure 5 Plot of $\log \frac{G^n}{t}$ versus $\frac{1}{T}$ for growth of nanocrystalline ZnO.

sintered at 973, 1073 and 1173 K. From the slopes of the lines, the grain growth kinetic exponents are 7, 6 and 4 for 973, 1073 and 1173 K respectively. The average value of *n* is around 6, which is obviously different from that of the coarse crystalline ZnO, for which the grain growth kinetic exponent is basically constant and approximately 3 in the temperature range from 1273 to 1673 K [3, 14]. Various grain growth kinetic exponents imply that the rate of grain growth of nano-materials is much more sensitive to the temperature than that of coarse crystalline materials. This agrees with the re-
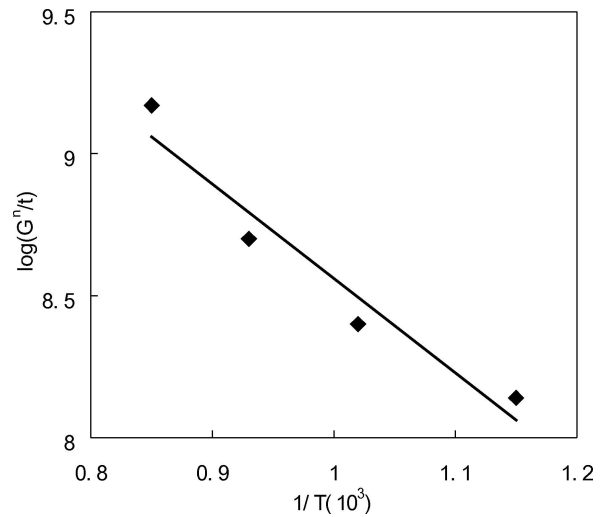
sults of microstructure observations. And large grain growth kinetic exponent also indicates that the sintering mechanism of nano-materials is more complex. It may be controlled by several mechanisms, which is not clear up to now [15].

Equation 1 can also be changed into another form as:

$$\log \frac{G^n}{t} = \frac{-0.434E}{R} \frac{1}{T} + \log D \qquad (3)$$

From the slope of the line of $\log \frac{G^n}{t}$ versus $\frac{1}{T}$, as shown in Fig. 5, the apparent activation energy for the grain growth can be obtained. Data scattering exists because

the grain growth does not exactly ascribe to the 1/6 power to time at the selected temperatures. However, there generally exists a reasonably good liner relationship between log (G^6/t) and $1/T$, ranging from 973 to 1173 K. Thus, the apparent activation energy for grain growth is calculated to be 64 ± 6 kJ/mol from the slope of the fitted line in Fig. 5, approximately 1/4 of that for the coarse crystalline ZnO (224 ± 16 kJ/mol). From the same plot, the value of pre-exponential constant D is also determined to be 1.52×10^{12} nm^6 h^{-1}.

In summary, sintering behavior of ZnO powder with a mean grain size of 20 nm was investigated in air. From 973 to 1173 K, the grain growth kinetic exponent is about 6 and the apparent activation energy for grain growth in this temperature range is 64 ± 6 kJ/mol. In order to obtain a homogeneous size distribution without apparent crystal growth in the sintered ZnO sample, the sintering temperature and time should be in the ranges of 973 to 1073 K and 3–5 h respectively.

References
1. J. HAN, P. Q. MANTAS and A. M. R. SENOS, *J. Eur. Ceram. Soc.* **22** (2002) 49.
2. J. WONG, *J. Appl. Phys.* **51**(8) (1980) 445.
3. T. SENDA, *J. Am. Ceram. Soc.* **73**(1) (1990) 106.
4. Y. J. KIMA and D.W. KIMB, *Mater. Chem. Phys.* **82** (2003) 410.
5. H. H. HNG and L. HALIM, *Mater. Lett.* **57** (2003) 1411.
6. J. R. GROZA, *Nanostructure Mater.* **12** (1999) 987.
7. J. LEE and J. J. MASHEK, *et al., J. Mater. Res.* **10** (1995) 2295.
8. X. J. QIN and G. J. SHAO, in Proceedings of the "High Tech-2001" International Seminar, Krasnoysrsk, Russia, June 2001, edited by V. I. Korko and G. L. Granitskaya (Altai State Technical University, Krasnoysrsk 2001) p. 70.
9. R. M. GERMAN, "Powder Metallurgy Science" (MPIF, Princeton, 1997) p. 250.
10. R. P. LIU, T. VOLKMANN and D.M. HERLACH, *Acta Mater.* **4** (2001) 439.
11. R. P. LIU, W. K. WANG, D. LI and D.M. HERLACH, *Scripta Mater.* **41** (1999) 855.
12. R. P. LIU, *Chin. Phys. Lett.* **20** (2003) 1622.
13. R. P. LIU, D. M. HERLACH, M. VANDYOUSSEFI and A. L. GREER, *Metall. Mater. Trans.* **A 35** (2004) 1067.
14. J. HAN, P. Q. MANTAS and A. M. R. SENOS, *J. Eur. Ceram. Soc.* **20** (2000) 2753.
15. M. J. MAYO, *Inter. Mater. Rev.* **41** (1996) 385.